

# Experimental study on honeycomb reactor using methane via chemical looping cycle for solar syngas<sup>☆</sup>

Xiangyu Liu<sup>a,b</sup>, Hao Zhang<sup>a</sup>, Hui Hong<sup>a,\*</sup>, Hongguang Jin<sup>a</sup>

<sup>a</sup> Institute of Engineering Thermophysics, Chinese Academy of Sciences, Beijing 100190, PR China

<sup>b</sup> University of Chinese Academy of Sciences, Beijing 100049, PR China



## HIGHLIGHTS

- The kinetic description of the chemical looping process for syngas production in a honeycomb reactor is provided.
- The reaction behavior of chemical looping process of methane to hydrogen was studied experimentally.
- The methane conversion and syngas concentration were both improved compared with non-honeycomb fixed bed reactor.
- The honeycomb oxygen carrier has a good cyclic stability and the degradation of oxygen carrier regeneration could be delayed.

## ARTICLE INFO

### Keywords:

Syngas production  
Chemical looping process  
Honeycomb reactor

## ABSTRACT

The chemical looping process on honeycomb reactor for solar syngas is experimentally studied in this work, which is the key reaction of the liquid sunshine production process. The honeycomb reactor realizes the integration of oxygen carrier and reaction chamber. NiO is placed in the reactor as oxygen carrier and methane is introduced as fuel gas. The results show that, with the development of process, the major reaction in the reactor gradually changed from methane complete oxidation to methane partial oxidation. During the process, the methane conversion and outlet syngas concentration is affected by the methane flow and fractional oxidation. Under the optimal operating conditions, the methane conversion can be maintained more than 95% and the concentration of outlet syngas can be around 90%. Compared with non-honeycomb fixed bed reactor, the methane conversion increases by more than 20 percent point and the concentration of outlet syngas increases by about 10 percent point. In addition, oxygen carrier in honeycomb reactor shows excellent cyclic stability in 30 times experiments.

## 1. Introduction

When the consequences of the overuse of fossil fuels come, are we prepared to deal with them? Since the first industrial revolution, fossil fuels have been the primary source of global energy. Behind the exponential progress powered by fossil fuels are the potential of energy crisis and the environmental deterioration [1,2]. Nowadays, annual carbon dioxide emissions are about twice as much as that can be absorbed by nature [3]. If we continue to rely on fossil fuels, the resulting climate change and air pollution will threaten our life [4]. Sunlight is the most abundant source of energy on earth, and it can provide about 885 million TWh of energy in a year, surpassing other kinds of renewable energy by hundreds of times [5]. But it is hard to use it as

easily as you flip a switch due to the decentralization and discontinuity of solar [6]. If we want to capture, store sunlight and supply it as energy source, the key process is to convert it into a stable, storable, high-energy-density chemical fuel.

The liquid sunshine vision is increasingly appealing to researchers [7]. Liquid fuels are not difficult to transport and store, and it can be widely used with some improvements to existing infrastructures. Liquid sunlight is designed to convert sunlight into liquid fuels such as methanol. Methanol is an attractive candidate because of its wide application. There are no C-C bonds in methanol which can effectively reduce the greenhouse gas emission due to its low carbon to hydrogen ratio [7]. As the raw material of methanol production, the preparation of solar syngas is a key process in current researches [8–11].

<sup>☆</sup> The short version of the paper was presented at ICAE2019, Aug 12–15, Västerås, Sweden. This paper is a substantial extension of the short version of the conference paper.

\* Corresponding author.

E-mail address: [honghui@iet.cn](mailto:honghui@iet.cn) (H. Hong).

## Nomenclature

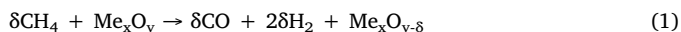
### Symbols

$a$	stoichiometric coefficient of the oxygen carrier
$B$	pressure efficiency
$C_{A0}$	concentration of the gaseous reactant in the gas bulk
$C_A^*$	equilibrium concentration of the gaseous reactant
$C_S$	concentration of solid reactant
$C_{S0}$	initial concentration of the solid reactant
$D_{eA}$	effective diffusivity of gaseous reactant in solid reactant
$D_{eA}$	effective diffusivity of gaseous reactant in product layer
$E$	activation energy
$H$	half the thickness of the solid between the two gas film
$h$	distance from the center of the solid reactant
$k_v$	parameter of reaction rate
$k_0$	Arrhenius reaction rate constant
$l$	length of the oxygen carrier along the direction of gas flow

$m_i$	mass of Species $i$
$M_O$	molar mass of oxygen
$n_i$	mole amounts of species $i$
$P$	reaction pressure inside the reactor during the reaction
$R_g$	molar gas constant
$r_0$	oxygen transfer rate
$T$	reaction temperature
$u_i$	moles consumed per unit time of species $i$
$w$	width perpendicular to the direction of gas flow
$X$	fractional oxidation
$\alpha_i$	number of oxygens required per mole of species $i$
$\beta$	geometry coefficient
$\eta$	conversion rate of methane
$\xi$	dimensionless distance
$\xi_m$	dimensionless distance of the boundary between product layer and solid reactant
$\phi$	Thiele modulus
$\rho$	molar density of the active component in oxygen carriers

Generally, solar syngas can be derived from water and fossil fuels by the processes of solar thermolysis, solar gasification, solar reforming and solar thermochemical cycle and so on [1]. The single-step thermal splitting of water or CO<sub>2</sub> is the simplest reaction to produce hydrogen and CO conceptually, but the extremely high temperature need of more than 2200 °C is impractical, which would result in a large number of thermal radiation losses and present a challenge to the materials [12,13]. To reduce the temperature of solar syngas preparation process, employing reducing reactant or hydrocarbon materials is considered an alternative approach [14–17]. Solar coal gasification process uses carbon to react with water to form CO and hydrogen. Due to the addition of coal, the temperature of hydrogen production from water can be reduced, but still higher than 1000 °C [18]. Solar methane-steam reforming is currently the most widely used method for preparing solar thermal fuels. Natural gas is fed to react with steam to produce syngas with the catalytic action of nickel. The reaction temperature can be reduced to around 900 °C [19]. If the reaction pressure is increased to 14 atm, the methane steam reforming can be achieved at around 800 °C [20]. But the temperature is not low enough to avoid excessive heat loss and heat resistance requirements of the materials, which would result in the limitation of working conditions restricts the combination with concentrated solar energy. To reduce the reaction temperature even further and realize the combination with low concentration ratio solar collector, chemical looping process gradually attracts attention and gradually becomes the most promising way of solar syngas production [21]. Chemical looping process is taken into account as a potential method for the production of syngas or hydrogen at lower temperature [22–24]. This process involves the use of oxygen carrier to implement the redox cycle for the syngas production [25].

Chemical looping process is a two-step redox cycle consisting of the partial oxidation of methane which is an endothermic reaction and the regeneration of oxygen carrier which is an exothermic reaction [26]. The schematic diagram of solar thermal fuel production via chemical looping process is displayed in Fig. 1. These two steps reactions are given by Eqs. (1) and (2), respectively [27].



Solar heat could be used as the heat source for the chemical looping syngas production. By means of the chemical looping process, the upgrade of solar energy to chemical energy is completed. The introduction of oxygen carrier as the oxidant of methane may eliminate the requirements for the temperature and pressure conditions of methane partial oxidation. It could provide a potential to produce syngas at

temperature lower than the reactions without oxygen carrier. Since the chemical looping process was proposed by Ishida and Jin [28], after many years of exploration, there has been some progress on chemical looping process. Methane conversion can be achieved at 98% during the chemical looping reforming of methane in the temperature range of 800–900 °C [29]. The reaction of Fe<sub>3</sub>O<sub>4</sub> with CH<sub>4</sub> was examined at 1 atm and above 1000 °C by Steinfeld et al., which could offer production of syngas from nature gas [30]. The chemical looping methane reforming for hydrogen and syngas production were also investigated using iron-based oxygen carrier, and the reaction kinetics of reduction and oxidation was determined [31].

For better solar fuels production performance, the reactivity of oxygen carrier plays an important role in the chemical looping process. A suitable oxygen carrier should have high conversion rate, high cycling stability and high mechanical strength. A variety of metal oxides including Fe, Mn, Ni, and Cu have been tested as oxygen carriers [32]. Their reactivities were compared in a fluidized bed reactor, and the results show that the reactivities with methane were in the order NiO > CuO > Mn<sub>2</sub>O<sub>3</sub> > Fe<sub>2</sub>O<sub>3</sub>. At 800 °C, only when NiO is used as oxygen carrier, the concentration of syngas at the outlet can reach more than 90%, and the rest cannot exceed 20%. If the reaction temperature rises to 850 °C, the use of Mn- and Cu-based oxygen carriers can lead to the peak concentration of syngas reaching more than 50% and 60%, respectively [33]. But Cu has a fairly low melting point at 1085 °C,

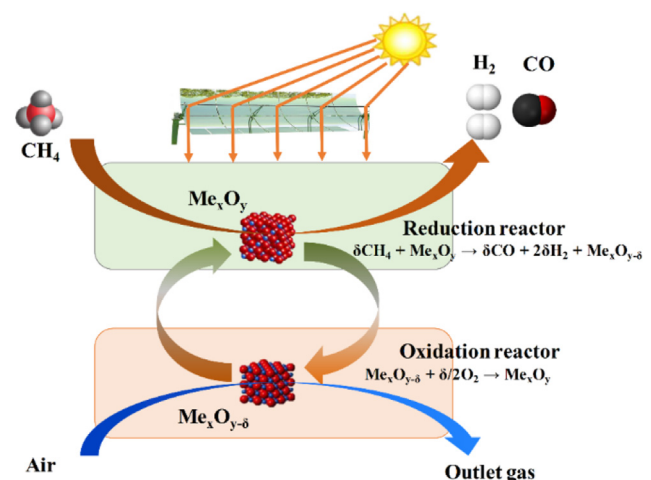


Fig. 1. Schematic diagram of solar syngas production via chemical-looping cycle.

which may cause agglomeration during the successive cycles [34]. Fe-based oxygen carrier has the advantages such as its low cost and environmental compatibility. By using this oxygen carrier, the maximum concentration of product gas can be about 70% at 950 °C [33]. Among them, Ni-based metal oxide exhibits a lower reaction temperature with methane and good catalytic effect of its reduction products on the reaction of methane and steam [29,35], which could also improve the performance of solar thermal fuel production. NiO is commonly supported by Al<sub>2</sub>O<sub>3</sub> to improve stability, thermal strength and mechanical strength [36,37]. During the regeneration of oxygen carrier, a large amount of heat can be released at high temperature of 1200 °C steadily and continuously [38].

The syngas production performance is closely related to reaction kinetics and reaction selectivity, and these two parameters are further determined by the distribution of oxygen carrier and contact condition of the gas-solid reactants [39]. It means that an excellent reactor configuration design is a vital requirement of chemical looping process. Lyngfelt proposed the utilization of fluidized bed reactor in the chemical looping reactor [40]. A 10 kW interconnected fluidized bed reactor was designed and established for studying the key reactions of chemical looping process. Due to the supply of a satisfactory gas-solid contact environment, fluidized bed reactor is most concerned and a series of fluidized bed reactor were constructed afterwards for chemical looping process [41–45]. However, a long gas-solid contact time in fluidized bed reactor needs a large size of the device. Also, in the fluidized bed reactor, redox cycle is driven by the circulating flow of the solid oxygen carrier. If solar heat is prepared to be the heat source for the endothermic reaction, it is hard to make the combination with the solar collector. Compare that, the fixed bed reactor may be more suitable for the chemical looping process driven by solar heat. With the assistance of the fixed bed chemical looping reactor, the reaction reactivity was experimental tested by using NiO and CoO [28]. Antzara et al. evaluate the performance of NiO oxygen carrier with several kinds of supporting materials [46]. But these earlier researches on common fixed bed reactor always indicate that, due to the limited diffusion of gas through the solid oxygen carriers, the value of conversion is limited to reach the required height. So, exploring a new kind of fixed bed reactor to improve gas-solid contact environment is the key progress. In our previous work, a novel honeycomb fixed-bed reactor for chemical-looping cycles was constructed [38,39]. In this reactor, oxygen carrier was integrated into the honeycomb chamber, which could improve the reaction rate and the conversion of the reactants [38]. Three kinds of honeycomb microchannel shapes were designed, and the experiments show that differences in the shapes bring about differences in specific surface area and porosity. In this study, the kinetics of the key reaction in solar syngas production is described and the reaction process is explored experimentally. NiO/Al<sub>2</sub>O<sub>3</sub> is selected as the oxygen carrier material to be processed into the honeycomb chamber with triangle microchannels. Moreover, the cycle reaction stability of honeycomb oxygen carrier was studied experimentally for the future design of solar chemical looping reactor.

## 2. Experimental section

### 2.1. Experimental bench

Based on the solar chemical looping process using methane and NiO to produce solar syngas, an experimental bench of honeycomb chemical looping reactor was designed and manufactured for studying the key reactions of the process. The schematic diagram of the experimental bench is shown in Fig. 2. The experimental bench is made of several mass flow controllers, an evaporator, a gas mixer, a preheater, a honeycomb reactor, a heat recover and a gas analyzer. Similar with fixed-bed reactor, this experimental bench has only one reactor to do the endothermic reaction of partial oxidation of methane and the exothermic reaction of the regeneration of oxygen carrier. The changes of

the reactions depend on the switching of the feed gas. Between the two reactions, inert gas is fed to avoid the meeting of air and methane. Honeycomb chamber is placed in a quartz glass tube covered with the adiabatic layer outside, and the temperature in honeycomb chamber is detected by the thermocouple. The honeycomb chamber is made by oxygen carrier, which realizes the integration of the oxygen carrier and reaction chamber (see Fig. 3).

### 2.2. Experimental materials

NiO is selected as the active component of oxygen carrier with Al<sub>2</sub>O<sub>3</sub> doped into as the inert support material. The corresponding mass ratio of NiO to Al<sub>2</sub>O<sub>3</sub> is 3:2. Based on this ratio, Al(NO<sub>3</sub>)<sub>3</sub>·9H<sub>2</sub>O and Ni(NO<sub>3</sub>)<sub>2</sub>·6H<sub>2</sub>O are weighed and dissolved in the mixture of isopropanol and water. Stirring the solution for 1 h, then dry it at 80 °C for 12 h, at 150 °C for 24 h and at 200 °C for 5 h in a drying oven. NiO/Al<sub>2</sub>O<sub>3</sub> powders can be obtained after 3 h calcination at 500 °C. The obtained powders are mixed with Kaolin, cellulose, oil, and deionized water, then the mixture slurry is stalled at 15 °C for 12 h. The required honeycomb pore shape and size is made and drying at 150 °C. Last, the final honeycomb oxygen carrier product is obtained after calcining in a muffle furnace at 1300 °C for 6 h [38].

Oxygen carrier materials are made into cylindrical monolithic blocks with series of axial microchannels. These microchannels provide sufficient passages for the feed gas, guaranteeing adequate contact of gas and solid reactants [39]. The properties of NiO/Al<sub>2</sub>O<sub>3</sub> honeycomb oxygen carrier are shown in Table 1.

### 2.3. Experimental setup

During the endothermic reaction, methane is introduced into the honeycomb reactor at 300–600 ml/min, and the reaction temperature is maintained at 600 °C. During the oxygen carrier regeneration stage, air is fed at 1200 °C. The processes are all controlled by an integrated controller and operated at one atmospheric pressure.

The experimental data is analyzed based on the composition of gas at the reactor outlet, which is collected and detected by gas chromatography.

During the partial oxidation of methane, oxygen is released from the lattice of NiO and it is recovered in the form CO, CO<sub>2</sub> and H<sub>2</sub>O. The oxygen transfer rate is calculated by:

$$r_0 = M_O \times (\alpha_{CO} \times u_{CO} + \alpha_{H_2O} \times u_{H_2O} + \alpha_{CO_2} \times u_{CO_2}) \quad (3)$$

where  $M_O$  is the molar mass of oxygen,  $\alpha_{CO}$  and  $\alpha_{H_2}$  are the number of oxygens required per mole of CO and H<sub>2</sub> to convert from reactant to product,  $u_{CO}$  and  $u_{H_2}$  are the moles consumed per unit time of CO and

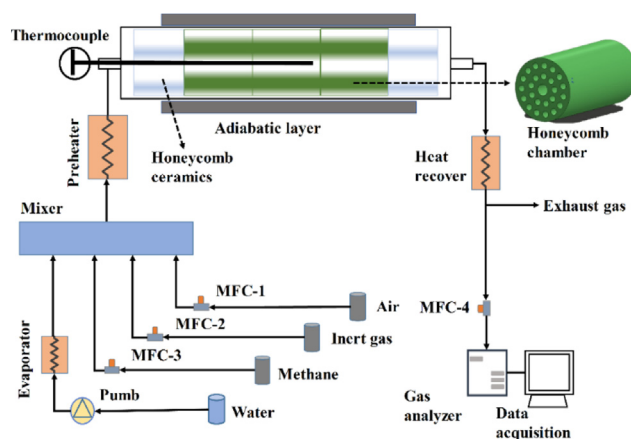


Fig. 2. Schematic diagram of the experimental bench of honeycomb chemical looping reactor.

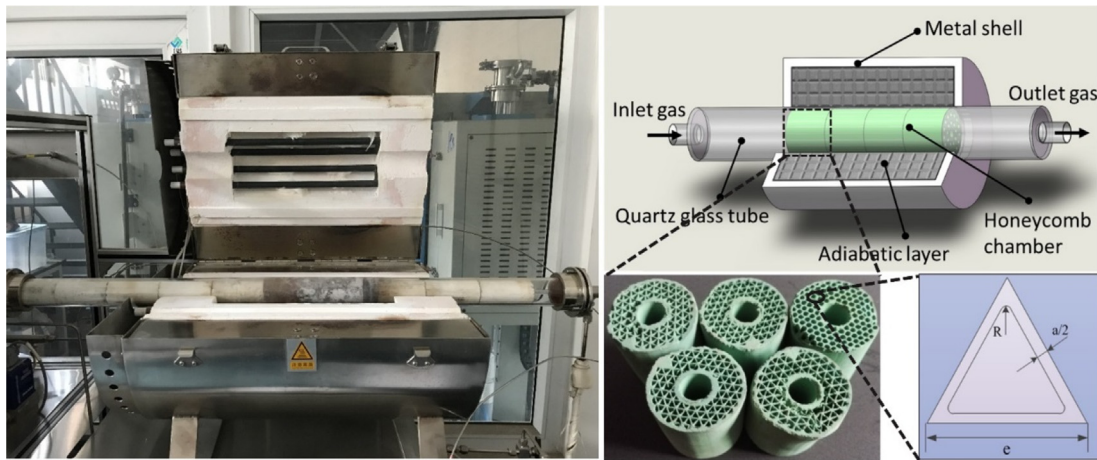


Fig. 3. The configuration diagram for the reactor and the honeycomb chamber.

Table 1

The properties of NiO/Al<sub>2</sub>O<sub>3</sub> honeycomb oxygen carrier.

	Unit	Value
Content of NiO	%	60
Microchannels shape		Triangle
Microchannel area	mm <sup>2</sup>	1.16
Surface area	mm <sup>2</sup> /mm <sup>3</sup>	2898
Wall thickness between two pores	mm	0.5
Center distance	mm	2.5
Total packing length	mm	120
Diameter	mm	36
Porosity		0.43

H<sub>2</sub>.

Fractional oxidation is a nondimensional indicator that indicates the conversion of oxygen carrier and it is defined as:

$$X = \frac{m_{ox} - m}{m_{ox} - m_{red}} \quad (4)$$

where  $m$  is the instantaneous mass of the oxygen carrier, and  $m_{ox}$  and  $m_{red}$  represent the mass of the oxygen carrier in a completely oxidized and reduced state, respectively.

The conversion rate of methane is an important index to measure the reaction performance, which could be calculated by:

$$\eta = \frac{n_{CO} + n_{CO_2} + n_C}{n_{CO} + n_{CO_2} + n_C + n_{CH_4}} \quad (5)$$

where the  $n_i$  is the mole amounts of species  $i$ .

#### 2.4. Experimental kinetic basis

The chemical looping process using methane and NiO is a solid-gas reaction. For this kind of solid-gas reaction process, most of the kinetic analysis is based on the homogeneous model or unreacted-core shrinking model [34]. In actuality, the research of Ishida shows that the majority of solid-gas reactions could not be described completely by both kinetic models, but may suit a versatile model displaying the intermediate of these two models [47]. Unlike the common granular oxygen carriers, honeycomb oxygen carrier is considered to be plate-like geometry types. The kinetic model of honeycomb oxygen carrier is described based on the plate-like geometry. During the reaction, the gaseous reactants would diffuse into the solid when the solid-gas contact occurs. In the honeycomb reactor, the diffusion of the gas reactants can be described as a stratified horizontal push flow from the gas-solid contact surface towards the interior of the solid. The gas is rapidly diffused throughout the oxygen carrier. The reactions occur

simultaneously from the gas-solid interface to the solid interior. This period is considered as the first stage reaction. Due to the nonnegligible diffusion resistance, the concentration of the gas inside the oxygen carrier is not uniform. The gas concentration decreases from the gas film to the solid intermediate layer. The active oxygen carrier on the solid outer surface is consumed faster than that in the bulk of the solid. After a period of reaction, the product layer is formed near the boundary of gas and solid, and it gradually invaded from the edge to the center. This period is considered as the second stage reaction. The schematic diagram is shown in Fig. 4.

The kinetic models are based on the following two assumptions: one is to apply the pseudo steady state approximation of the gas reactants, and the other one is that the reaction rate is linearly dependent on the concentration of the gaseous reactants [47]. During the chemical looping process, the fractional oxidation could be obtained by

$$X = \frac{\int_0^H lwC_S dh}{\int_0^H lwC_{S0} dh} \quad (6)$$

where  $C_S$  is the concentration of solid reactant at the distance of  $h$  from the solid center;  $h$  is the distance from the center of the solid reactant;  $H$  is half the thickness of the solid between the two gas film;  $C_{S0}$  is the initial concentration of the solid reactant;  $l$  is the length of the oxygen carrier along the direction of gas flow, which is expressed as the axial length of the oxygen carrier macroscopically;  $w$  is the width perpendicular to the direction of gas flow, which is expressed as the cross-section circumference of the axial microchannels of honeycomb oxygen carrier macroscopically. If the diffusion resistance in the gas film around the solid reactant is considered small enough to be negligible, the consumption rate of oxygen carrier deduced based on the material balance in the first stage reaction could be expressed as:

$$\frac{dC_S}{dt} = -k_v C_{S0} (C_{A0} - C_A^*) \frac{\sinh(\phi\xi)}{\xi \sinh(\phi)} \quad (7)$$

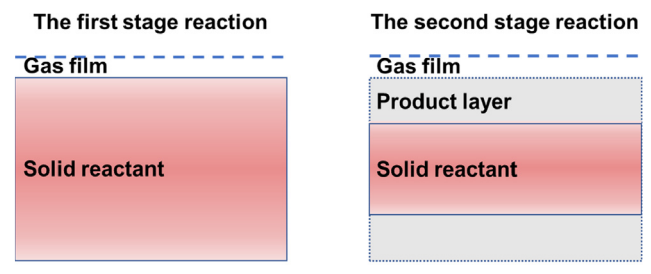


Fig. 4. The schematic diagram of the two-stage kinetic model.

where  $C_{A0}$  is the concentration of gaseous reactant in the gas bulk;  $C_A^*$  is the equilibrium concentration of gaseous reactant;  $\xi$  is the dimensionless distance, and  $\phi$  is the Thiele modulus. The definition equations of  $\xi$  and  $\phi$  are shown as follows:

$$\xi = h/H \quad (8)$$

$$\phi = R \sqrt{\frac{ak_v C_{S0}}{D_{eA}}} \quad (9)$$

where  $a$  is the stoichiometric coefficient of the oxygen carrier;  $D_{eA}$  is the effective diffusivity of gaseous reactant in solid reactant;  $k_v$  is the parameter of reaction rate which could be described in chemical looping process as [38]:

$$k_v = k_0 \left(\frac{P}{P_0}\right)^{-b} \frac{a}{\rho} \exp\left(\frac{-E}{R_g T}\right) (X_0 - X)^\beta \quad (10)$$

where  $k_0$  is the Arrhenius reaction rate constant at atmospheric pressure  $P_0$ ;  $P$  is the reaction pressure inside the reactor during the reaction;  $b$  is the pressure efficiency, which represents the effect of the pressure;  $\rho$  is the molar density of the active component in oxygen carriers;  $E$  is the activation energy of the reaction;  $\beta$  is the geometry coefficient;  $R_g$  is the molar gas constant and  $T$  is the reaction temperature. In the second stage reaction, the consumption rate of oxygen carrier could be expressed as:

$$\frac{dC_S}{dt} = -k_v C_{S0} \frac{(C_{A0} - C_A^*)}{1 + \frac{D_{eA}}{D_{eA}}(1 - \xi_m)[\phi \xi_m \coth(\phi \xi_m) - 1] \sinh(\phi \xi)} \frac{\xi_m \sinh(\phi \xi)}{\xi} \quad (11)$$

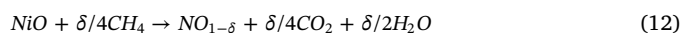
where  $D_{eA}$  is the effective diffusivity of gaseous reactant in product layer;  $\xi_m$  is the dimensionless distance of the boundary between product layer and solid reactant. During the chemical looping process, methane could be converted almost completely. So the equilibrium concentration of methane could be considered as 0.

### 3. Result and discussion

#### 3.1. Reaction behavior in honeycomb chemical looping reactor

The experimental study on the honeycomb chemical looping reactor using methane and NiO/Al<sub>2</sub>O<sub>3</sub> was carried out. The reduction behavior of 213.5 g NiO/Al<sub>2</sub>O<sub>3</sub> at 600 °C in a stream of 500 ml/min methane is presented in Fig. 5. The concentrations of outlet gas were detected by the chromatography, and the results of the first 3000 s were selected as the basis for studying. During the reaction, the initial value of fractional

oxidation  $X$  is equal to 1 and the initial value of syngas is near 10% and that of CO<sub>2</sub> is about 90%. At this point, the oxygen content in the oxygen carrier is most abundant. According to our previous study [39], the higher the fractional oxidation, the faster the oxygen transfer rate can be provided by oxygen carrier. And with the reduction of fractional oxidation, the oxygen transfer rate would gradually decrease. At the beginning of the reaction, a stream of 500 ml/min methane passes through the honeycomb chamber in contact with oxygen carrier, and more than 20 mg/min oxygen transfer rate could be provided. Based on the mentioned kinetic model, the reaction process can be divided into two parts. At the beginning, the reaction is at the first stage of the kinetic model. At this period, methane rapidly diffuses into the oxygen carrier, and the reactions occur simultaneously throughout the whole oxygen carrier body from the outer surface to the center. Methane is in full contact with the entire oxygen carrier and obtains oxygen from the entire oxygen carrier, which results in the rapid transfer of oxygen from NiO to methane. The overall reaction rate depends on the oxygen transfer rate. Under the reaction conditions, oxygen transfer rate reached the maximum, and the maximum of that is related to the fractional oxidation. At this oxygen transfer rate about 90% of the methane can get enough oxygen to be oxidized completely to CO<sub>2</sub> and water. The main reaction occurring at this time is as follows:



As the reaction goes on, the concentration of syngas begins to increase and the concentration of CO<sub>2</sub> begins to decrease. After 700 s, the composition of syngas in the outlet gas exceeds that of CO<sub>2</sub>. The concentration of syngas continues to rise while the concentration of CO<sub>2</sub> continues to fall. And the reaction goes to 1200 s, the concentration of syngas is above 80% and tends to be stable, and the concentration of CO<sub>2</sub> would be less than 20%. At the region between 0 and 1200 s, the fractional oxidation reduces from 1 to around 0.5, and the oxygen transfer rate decreases from above 20 mg/min to around 10 mg/min. With the development of the reaction, oxygen carriers near the gas-solid contact boundary are the first to be completely depleted. The product layer gradually appears at the boundary. The reaction enters the second stage of the kinetic model. At this period, according to the Eq. (11) the reaction rate is not only related to the fractional oxidation, but also affected by the thickness of the product layer. The product layer gradually grows from the surface to the bulk of oxygen carrier, which leads to longer time and distance requirements for the diffusion of methane to the reaction layer. Increased diffusion resistance results in inadequate contact between methane and oxygen carrier, and the decrease of oxygen transfer rate. Less oxygen is transferred to react with methane. More methane is partially oxidized to form CO and hydrogen rather

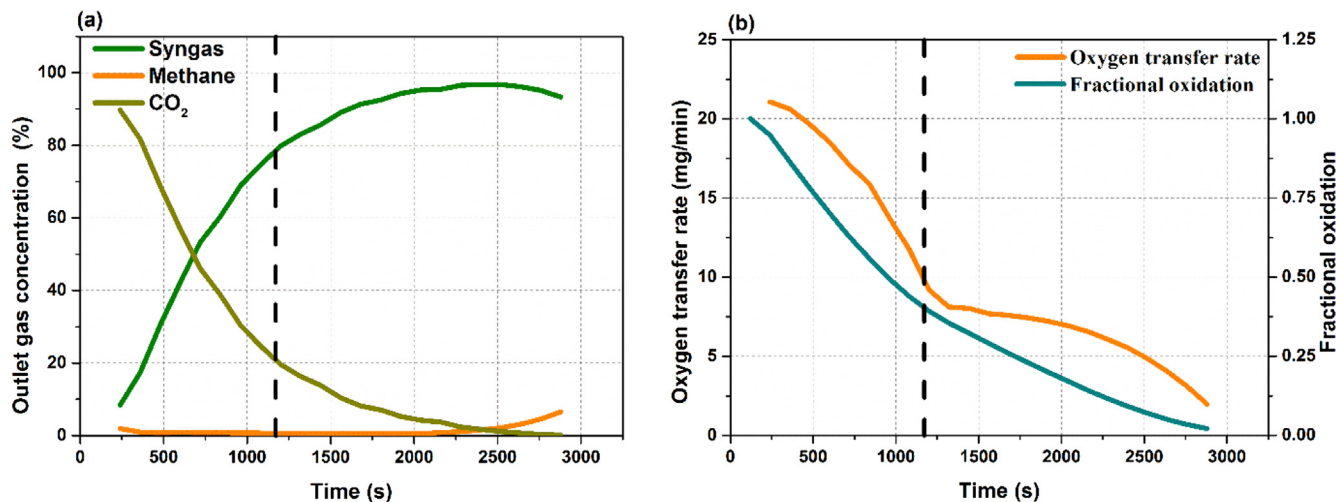


Fig. 5. (a) Outlet gas concentration during the reduction reaction, (b) oxygen transfer rate and fractional oxidation during the reduction reaction.

than completely oxidized before. The composition of the gas at the outlet of the reactor changed from CO<sub>2</sub> dominated to syngas dominated gradually. The equation of the methane partial oxidation is as follows:



During the reaction of oxygen carrier regeneration, inlet gas is switched to air, and inlet gas flow rate is increased to 3000 ml/min. The reactivity of this reaction process has been described in our previous studies [38,39]. An experimental phenomenon attracted our attention which is shown in Fig. 6. Water droplets gradually appeared in the reactor outlet pipe placed in the room temperature. Water vapor was carried out of the reactor by the outlet gas. This indicates that part of the water generated during the reduction reaction may be locked by the honeycomb reaction chamber and not be carried out during the reduction reaction. As the gas flow in the reactor increases several times, the water locked in the honeycomb reaction chamber is carried out by the air. The water generated by the inevitable complete oxidation of methane at the beginning of the reaction may always exist in the entire reduction process. As the reaction progresses, NiO is gradually reduced to Ni by methane. Nickel has a certain catalytic effect of such side reactions shown in Eqs. (14) and (15). With the consumption of nickel oxide, the nickel content is getting higher and higher, and the catalytic effect on these two reactions would be gradually enhanced.



As we know, carbon deposits would form on the surface of the oxygen carrier during the chemical looping reaction which is shown in Eq. (16). The formation of carbon deposits could adversely affect the performance of the oxygen carrier, and it is necessary to suppress the formation of carbon deposits during the chemical looping process. The presence of water can remove the carbon deposits on the oxygen carrier, which is shown in Eq. (17). The adverse influences of carbon deposits on the performance of oxygen carrier are also avoided. Additionally, the side reactions of Eq. (14)–(17) can produce hydrogen or CO without oxygen carrier consumption, which is also beneficial for syngas production. Therefore, the water generated from the complete oxidation of methane that cannot be avoided in the beginning of the reaction has beneficial effects on the production of chemical looping syngas.



In order to take advantage of the chemical looping cycles to syngas, the reaction in Eq. (13) is required to be the main reaction in the reactor. Especially when the chemical looping cycle is combined with solar energy that is used as the heat source of reduction reaction, the collected solar energy is best used to drive the conversion of methane into syngas rather than CO<sub>2</sub> and water. The reaction process in honeycomb reactor needs to be actively regulated.

### 3.2. Effect of the methane flow rate

Fig. 7 shows the effect of the methane flow rate on the reaction process in the honeycomb reactor. Fractional oxidation is a parameter representing the oxygen content in the oxygen carrier. The fractional oxidation value of 1 indicates that the oxygen content in the carrier is full, and the value of 0 indicates that the oxygen in the carrier is depleted. When the methane flow is 300 ml/min, under the condition that the fractional oxidation is above 0.2, the outlet gas concentration of syngas grows slowly and remains below 40%. After the fractional oxidation is below 0.2, the rise rate in syngas concentration is accelerated. The concentration of syngas barely reached 80% until the oxygen in oxygen carrier is almost completely depleted. When the methane flow is 500 ml/min, a reduction in fractional oxidation to 0.7 would allow the

concentration of syngas to exceed 40%. The highest syngas concentration could achieve at no less than 90%. By comparing the curve of 500 ml/min methane flow and the curve of 300 ml/min flow, the increase of methane flow could promote the partial oxidation of methane to produce syngas. At the same fractional oxidation, the syngas concentration at 500 ml/min inlet methane flow could be up to 50 percent points higher than that at 300 ml/min. With the expected syngas outlet content set above 60%, the available range of fractional oxidation is extended from 0 to 0.1 at 300 ml/min methane flow to 0–0.6 at 500 ml/min methane flow. This promotion could enlarge the activity range of oxygen carrier and reduce the cycle times of oxygen carrier in syngas production. With an increase in methane flow at the inlet, the oxygen transfer rate of oxygen carrier may hardly match the increase of oxygen demand for methane oxidation. Part of methane that can be thoroughly oxidized at lower flow rate could not get enough oxygen after the flow increases. More methane is partially oxidized into syngas instead of carbon dioxide with the increase of inlet methane flow. However, it is not always the case that increasing methane flow is beneficial for syngas production. When the methane inlet flow increased from 500 ml/min to 600 ml/min, the concentration of the syngas decreased with the same fractional oxidation. When the methane flow is set at 600 ml/min, fewer experimental sites were distributed in the area with fractional oxidation of 0.4–1. At the different methane flows, the measuring time interval between each test site is the same. It means that excess methane flowing through the oxygen carrier may lead to a rapid depletion of oxygen carrier at the beginning of the reaction. Although the concentration of syngas rises faster at 600 ml/min than that at 500 ml/min, the excess oxygen transfer allows more oxygen to be used to produce carbon dioxide and water at the start of the reaction.

In order to ensure the performance of syngas production from the chemical looping process, not only the high concentration of the syngas needs to be required, but also the conversion rate of methane needs to be guaranteed. In Fig. 7(b), the methane conversions of the reaction processes are shown. With the methane flow of 300 ml/min, methane conversion can be maintained above 95% until a transition occurs when the fractional oxidation is below 0.1. Once the value of fractional oxidation is below the turning point, the curve of methane conversion would change from steady to decline. With the increase of the methane flow, the turning point appears at a higher fractional oxidation. With the methane flow of 500 ml/min, the methane conversion starts to decline at the fractional oxidation of 0.1. Although the methane conversion decreases when the fractional oxidation is below 0.1, it can basically guarantee that conversion is above 70%. As the methane flow increases further to 600 ml/min, the turning point appears at a higher fractional oxidation of 0.2. As oxygen carrier is gradually consumed by



Fig. 6. Water carried out by the outlet gas during the reaction of oxygen carrier regeneration.

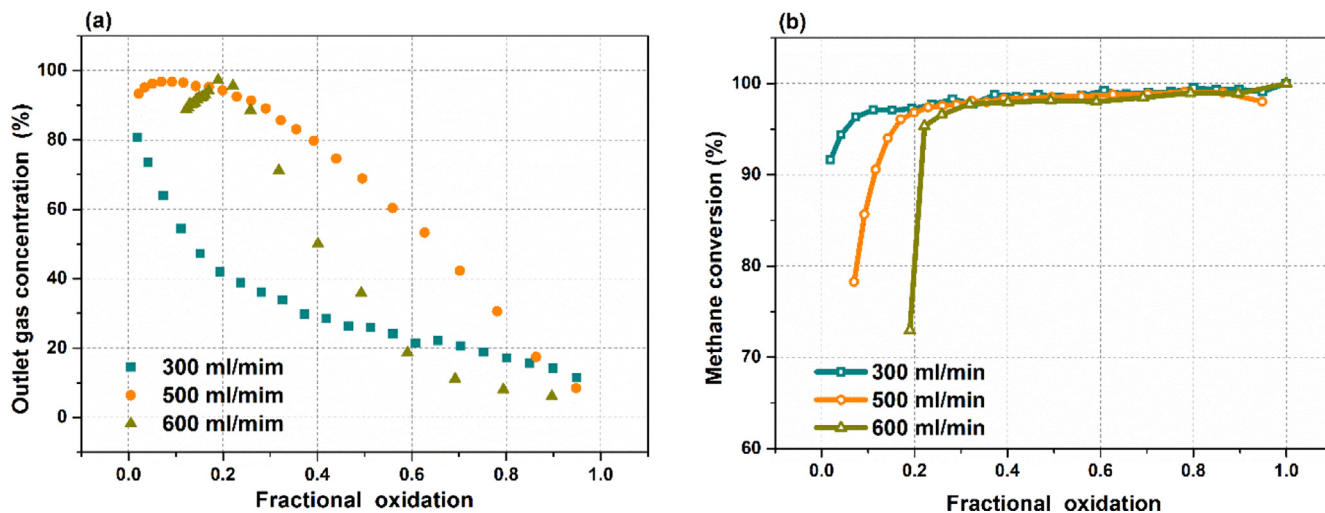


Fig. 7. Outlet syngas concentrations (a) and methane conversions (b) at different fractional oxidation when the methane flow is 300 ml/min, 500 ml/min, 600 ml/min.

methane, the fractional oxidation of the oxygen carrier decreases. Part of methane may be difficult to be diffused into the bulk of reaction chamber to be oxidized by unreacted oxygen carrier, causing the methane conversion to decrease. The higher the methane flow, the larger the amount of oxygen carrier required for the reaction, and the earlier the decline in methane conversion begins.

Comprehensively considering the concentration of syngas at the reactor outlet and the methane conversion, 500 ml/min may be the appropriate methane flow value in this reaction process. Decreasing methane flow will reduce the concentration of syngas produced by the reaction. Although reducing methane flow can increase methane conversion, the benefits are not significant. Further increasing methane flow will reduce the concentration of syngas also, and the methane conversion would be affected. Additionally, if the active range of the fractional oxidation is controlled between 0.1 and 0.6, not only will the methane conversion rate be guaranteed at no less than 80%, but also the syngas concentration will be maintained at no less than 60.

3.3. Evaluation of reaction performance

Compared with methane steam reforming, chemical looping process can effectively reduce the temperature and enable the process to be carried out under atmospheric pressure. Compared with the

conventional chemical-looping reforming, the use of honeycomb reactor enables the process to be carried out at a lower temperature with the similar output syngas.

The chemical looping process in honeycomb reactor is also compared that in non-honeycomb fixed bed reactor. The comparisons of methane conversion and outlet syngas concentration are shown in Fig. 8. The comparative experiments were carried out at 650 °C [46]. In non-honeycomb fixed bed reactor, methane conversions are always no more than 70%, and the effective product concentration is around 80%. The use of honeycomb reactor can improve the methane conversion to above 90%. Also, the syngas concentration is increased by up to 10 percent point, which would facilitate the separation and storage of syngas. These strengths are due to the porous structure of honeycomb reactor which provides better turbulence and enhances the gas-solid contact and diffusion of the gas in the body of oxygen carrier. And the ability of the honeycomb chamber to hold water allows CH<sub>4</sub> and CO to react with H<sub>2</sub>O as the side reactions, increasing the syngas production.

3.4. Cyclic stability of oxygen carrier

Good regeneration of oxygen carrier can effectively reduce the replacement frequency of oxygen carrier. It is an important factor to avoid extra cost in chemical looping process. Especially in the use of the

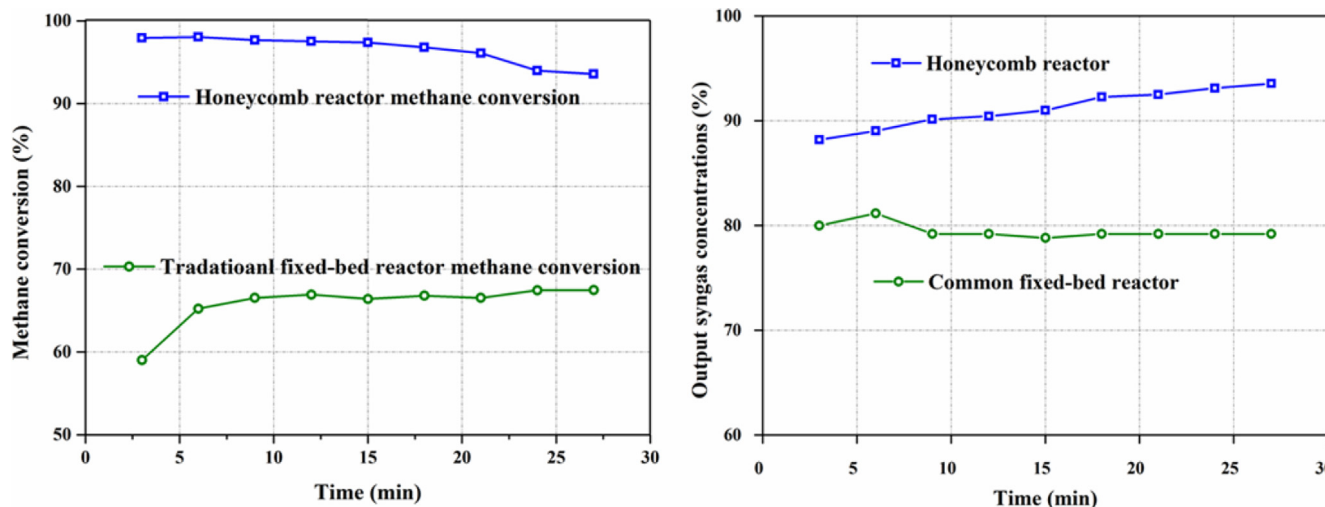


Fig. 8. Comparations of methane conversion and outlet syngas concentration between honeycomb chemical looping reactor and non-honeycomb fixed bed reactor.

chemical looping process combined with solar, high cyclic stability is also an essential requirement for the application of the chemical-looping cycles. Solar energy can only be used during the day but not at night. To adapt to this characteristic of solar energy, the chemical looping process could be repeated once a day. During the day, solar energy could be collected to be used as the heat source for the endothermic reduction reaction. And at night, thermal energy could be released by the oxidation reaction to drive the advanced power cycle. The cyclic performance of the oxygen carrier determines the frequency of oxygen carrier material replacement. Oxygen carrier material consumption is an important part of the cost of the chemical looping process. Therefore, excellent oxygen carrier cycle performance is essential for the solar chemical looping cycle process.

The comparison of oxygen carrier regeneration in the honeycomb reactor and a traditional fixed-bed reactor is shown in Fig. 9. Oxygen carrier was tested continuously both in the designed honeycomb reactor and fixed-bed reactor for 30 times continuous redox cycles. In non-honeycomb fixed-bed reactor, the fractional oxidation can just be reduced to about 0.6 [48], which means there are still 60% oxygen carrier that is hard to react with. Also, the variable range of fractional oxidation are uneven and gradually decays. Especially after 16 times cycle, the decay intensifies obviously. The available oxygen carrier in the reaction is less and less, and it is difficult to restore the oxygen carrier to the initial state in the regeneration process. But in honeycomb reactor, fractional oxidation can vary between 0 and 1. Oxygen carrier can be converted almost completely from the beginning to the end. The conversion of oxygen carrier remains unchanged during the 30 times cycle. The scanning electron microscope images of oxygen carrier are shown in Fig. 10. The pictures are taken at ten thousand times magnification on a micron scale. By comparing the oxygen carrier structures before and after 30 times cycles, it could be seen that the microstructure of oxygen carrier has no changes. Also, there is no obvious sintering on the oxygen carrier. The conclusion can be obtained that the chemical-looping hydrogen production process of honeycomb NiO/Al<sub>2</sub>O<sub>3</sub> has excellent stability and honeycomb reactor can delay the degradation of oxygen carrier regeneration.

### 3.5. Outlook

For the production of syngas or hydrogen, CH<sub>4</sub> is one of the main raw materials. Methane reforming technology is a relatively mature process for the production of syngas or hydrogen. To meet the heat absorption requirement of the methane reforming reaction, above 30% methane needs to be combusted [49]. This means that at most about 70% of methane can be converted into syngas, which results in the energy efficiency is limited. In addition, the combustion of methane

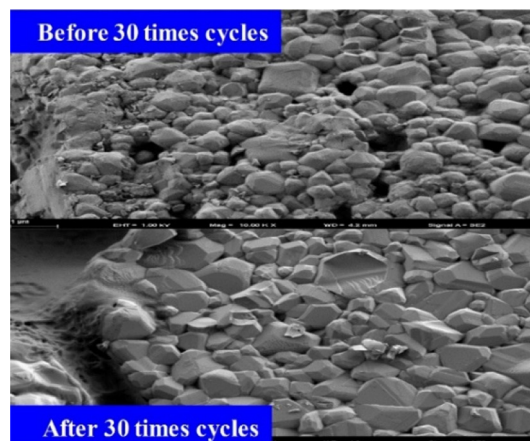


Fig. 10. Scanning electron microscope images of oxygen carrier before and after 30 times cycles at ten thousand times magnification of a micron scale.

produces hard-to-separated CO<sub>2</sub>. If CO<sub>2</sub> is not captured, it will aggravate the greenhouse effect. Capturing CO<sub>2</sub> in the tail gas after combustion requires the gas separation, and the energy consumption required is high. Therefore, it is necessary to develop a low-carbon syngas production process. The production of syngas by direct use of solar energy, such as solar driven water decomposition, can avoid the emission of CO<sub>2</sub>, but the reaction temperature is too high and the conversion rate is low, which limits the development potential. The chemical looping process with the complementarity of methane and solar energy is considered as the candidate. The use of solar energy is expected to reduce the consumption of methane used to be burn off heat, which would improve the energy conversion efficiency in the process of making syngas from methane. Compared with methane reforming, chemical looping process can avoid the separation and capture processes of CO<sub>2</sub>, enabling clean, efficient and low-carbon conversion of methane. Also, the reaction temperature can be reduced, which benefits the coupling with concentrated solar collectors. The reaction temperature is higher, the requirement for concentrated solar collector is higher. The investment cost will increase with the addition of concentrated solar collector. But the cost of CO<sub>2</sub> separation and capture can be avoided in chemical looping process, and the decrease of reaction temperature will reduce the construction and operation cost of concentrated solar collector. Therefore, the economy of solar driven chemical looping process using methane has the development potential.

The use of solar energy is essential to consider the impact of solar instability, especially the impact on the oxygen carrier. The instability of solar heat may cause heat flow instability in the reaction process. In

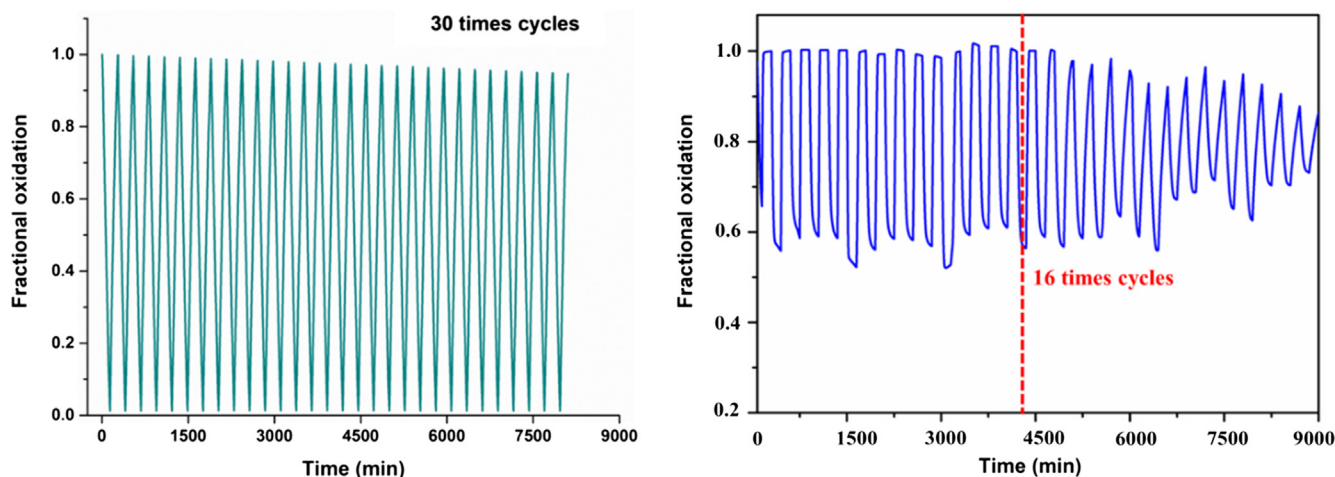


Fig. 9. Cyclic stability of oxygen carrier in honeycomb reactor and traditional fixed-bed reactor.

the future work, the reactivity and sintering resistance of oxygen carrier under unstable heat flow conditions may be the focus to be paid attention. In addition, the current heat transfer method of chemical looping reactor is indirect, which needs heat transfer media such as molten salt or thermal oil to transfer the collected solar heat. In this way, the heat resistance of the heat transfer process is large and the heat loss is large too. Perhaps a better approach would be to develop the direct solar chemical looping reactor, which may be a chamber reactor that can transmit solar light directly and can be integrated with a solar collector. By using this kind of reactor, additional thermal conductivity may be avoided and energy utilization efficiency has the potential to be improved.

#### 4. Conclusions

In this work, the chemical looping process using methane for syngas production is experimentally analyzed in a honeycomb reactor. NiO/Al<sub>2</sub>O<sub>3</sub> is selected as the oxygen carrier and the reaction temperature is conducted at 600 °C. With the development of chemical looping process, the major reaction changes from the complete oxidation of methane to the partial oxidation of methane. This means that in order to obtain syngas as the product, the fractional oxidation needs to be maintained within the optimal range. So that the oxygen transfer rate is not too fast to completely oxidized the methane. An increase in the inlet flow of methane can effectively increase the concentration of the outlet syngas. But excessive increase in methane flow would have the opposite effect on syngas production, with a simultaneous decrease in methane conversion. In addition, the honeycomb reactor shows a better reaction performance than non-honeycomb reactor. Under the optimal operating conditions, the methane conversion and outlet syngas concentration in the honeycomb reactor increased by 20 percent points and 10 percent point respectively compared with the non-honeycomb reactor. The honeycomb oxygen carrier also shows excellent cyclic stability in 30 times experiments.

#### Acknowledgement

The authors gratefully acknowledge the support of the Basic Science Center Program for Ordered Energy Conversion of the National Natural Science Foundation of China (No. 51888103), the National Natural Science Foundation of China (Grant No. 51590904), and the Chinese Academy of Sciences Frontier Science Key Research Project (QYZDY-SSW-JSC036).

#### References

- Meier A, Steinfeld A. Solar thermochemical production of fuels. *Adv Sci Technol* 2011;74:303–12.
- Lilliestam J, Labordena M, Patt A, Pfenninger S. Empirically observed learning rates for concentrating solar power and their responses to regime change. *Nat Energy* 2017;2:17094.
- IPCC. Climate Change 2014: Synthesis Report. Contribution of Working Groups I, II and III to the Fifth Assessment Report of the Intergovernmental Panel on Climate Change. IPCC; 2014.
- Romero M, Steinfeld A. Concentrating solar thermal power and thermochemical fuels. *Energy Environ Sci* 2012;5:9234–45.
- Solar Energy Perspectives. International Energy Agency; 2011.
- Chuayboon S, Abanades S, Rodat S. Syngas production via solar-driven chemical looping methane reforming from redox cycling of ceria porous foam in a volumetric solar reactor. *Chem Eng J* 2019;356:756–70.
- Shih CF, Zhang T, Li J, Bai C. Powering the future with liquid sunshine. *Joule* 2018;2:1925–49.
- Steinfeld A. Solar thermochemical production of hydrogen—a review. *Sol Energy* 2005;78:603–15.
- Navarro RM, Peña MA, Fierro JLG. Hydrogen production reactions from carbon feedstocks: fossil fuels and biomass. *Chem Rev* 2007;107:3952–91.
- Turner JA. Sustainable hydrogen production. *Science* 2004;305:972–4.
- Svoboda K, Siewiorek A, Baxter D, Rogut J, Pohořelý M. Thermodynamic possibilities and constraints for pure hydrogen production by a nickel and cobalt-based chemical looping process at lower temperatures. *Energy Convers Manage* 2008;49:221–31.
- Agrafiotis C, Roeb M, Sattler C. A review on solar thermal syngas production via redox pair-based water/carbon dioxide splitting thermochemical cycles. *Renew Sustain Energy Rev* 2015;42:254–85.
- Abanades S, Charvin P, Flamant G, Neveu P. Screening of water-splitting thermochemical cycles potentially attractive for hydrogen production by concentrated solar energy. *Energy* 2006;31:2805–22.
- Brkic M, Koepf E, Meier A. Solar carbothermal reduction of aerosolized ZnO particles under vacuum: modeling, experimentation, and characterization of a drop-tube reactor. *Chem Eng J* 2017;313:435–49.
- Levêque G, Abanades S. Thermodynamic and kinetic study of the carbothermal reduction of SnO<sub>2</sub> for solar thermochemical fuel generation. *Energy Fuels* 2013;28:1396–405.
- Kräupl S, Frommherz U, Wieckert C. Solar carbothermic reduction of ZnO in a two-cavity reactor: laboratory experiments for a reactor scale-up. *J Sol Energy Eng* 2006;128:8–15.
- Osinga T, Frommherz U, Steinfeld A, Wieckert C. Experimental investigation of the solar carbothermic reduction of ZnO using a two-cavity solar reactor. *J Sol Energy Eng* 2004;126:633–7.
- Lin S, Harada M, Suzuki Y, Hatano H. Hydrogen production from coal by separating carbon dioxide during gasification. *Fuel* 2002;81:2079–85.
- Kathe MV, Empfield A, Na J, Blair E, Fan L-S. Hydrogen production from natural gas using an iron-based chemical looping technology: thermodynamic simulations and process system analysis. *Appl Energy* 2016;165:183–201.
- Barelli L, Bidini G, Gallorini F, Servili S. Hydrogen production through sorption-enhanced steam methane reforming and membrane technology: a review. *Energy* 2008;33:554–70.
- Marxer D, Furler P, Takacs M, Steinfeld A. Solar thermochemical splitting of CO<sub>2</sub> into separate streams of CO and O<sub>2</sub> with high selectivity, stability, conversion, and efficiency. *Energy Environ Sci* 2017;10:1142–9.
- Dai XP, Wu Q, Li RJ, Yu CC, Hao ZP. Hydrogen production from a combination of the water – gas shift and redox cycle process of methane partial oxidation via lattice oxygen over LaFeO<sub>3</sub> Perovskite Catalyst. *J Phys Chem B* 2006;110:25856–62.
- Dai XP, Li J, Fan JT, Wei WS, Xu J. Synthesis gas generation by chemical-looping reforming in a circulating fluidized bed reactor using perovskite LaFeO<sub>3</sub>-based oxygen carriers. *Ind Eng Chem Res* 2012;51:11072–82.
- Fan L-S, Li F. Chemical looping technology and its fossil energy conversion applications. *Ind Eng Chem Res*. 2010;49:10200–11.
- Lu C, Li K, Wang H, Zhu X, Wei Y, Zheng M, et al. Chemical looping reforming of methane using magnetite as oxygen carrier: structure evolution and reduction kinetics. *Appl Energy* 2018;211:1–14.
- Jiang Q, Zhang H, Cao Y, Hong H, Jin H. Solar hydrogen production via perovskite-based chemical-looping steam methane reforming. *Energy Convers Manage* 2019;187:523–36.
- Akbari-Emadabadi S, Rahimpour M, Hafizi A, Keshavarz P. Production of hydrogen-rich syngas using Zr modified Ca-Co bifunctional catalyst-sorbent in chemical looping steam methane reforming. *Appl Energy* 2017;206:51–62.
- Ishida M, Jin HG. A new advanced power-generation system using chemical-looping combustion. *Energy* 1994;19:415–22.
- Luis F, Ortiz M, García-Labiano F, Adánez J, Abad A, Gayán P. Hydrogen production by chemical-looping reforming in a circulating fluidized bed reactor using Ni-based oxygen carriers. *J Power Sources* 2009;192:27–34.
- Steinfeld A, Kuhn P, Karni J. High-temperature solar thermochemistry: production of iron and synthesis gas by Fe<sub>3</sub>O<sub>4</sub>-reduction with methane. *Energy* 1993;18:239–49.
- Go KS, Son SR, Kim SD. Reaction kinetics of reduction and oxidation of metal oxides for hydrogen production. *Int J Hydrog Energy* 2008;33:5986–95.
- Zafar Q, Mattisson T, Gevert B. Integrated hydrogen and power production with CO<sub>2</sub> capture using chemical-looping reforming redox reactivity of particles of CuO, Mn<sub>2</sub>O<sub>3</sub>, NiO, and Fe<sub>2</sub>O<sub>3</sub> using SiO<sub>2</sub> as a support. *Ind Eng Chem Res* 2005;44:3485–96.
- Forutan H, Karimi E, Hafizi A, Rahimpour M, Keshavarz P. Expert representation chemical looping reforming: a comparative study of Fe, Mn, Co and Cu as oxygen carriers supported on Al<sub>2</sub>O<sub>3</sub>. *J Ind Eng Chem* 2015;21:900–11.
- Adanez J, Abad A, García-Labiano F, Gayán P, de Diego LF. Progress in Chemical-looping combustion and reforming technologies. *Prog Energy Combust Sci* 2012;38:215–82.
- Tang M, Xu L, Fan M. Progress in oxygen carrier development of methane-based chemical-looping reforming: A review. *Appl Energy*. 2015;151:143–56.
- Mattisson T, Järnäs A, Lyngfelt A. Reactivity of Some metal oxides supported on alumina with alternating methane and oxygen application for chemical-looping combustion. *Energy Fuels* 2003;17:643–51.
- Mattisson T, Johansson M, Lyngfelt A. The use of NiO as an oxygen carrier in chemical-looping combustion. *Fuel* 2006;85:736–47.
- Zhang H, Hong H, Jiang Q, Deng Yn, Jin H, Kang Q. Development of a chemical-looping combustion reactor having porous honeycomb chamber and experimental validation by using NiO/NiAl<sub>2</sub>O<sub>4</sub>. *Appl Energy* 2018;211:259–68. <https://doi.org/10.1016/j.apenergy.2017.11.053>.
- Zhang H, Liu X, Hong H, Jin H. Characteristics of a 10 kW honeycomb reactor for natural gas fueled chemical-looping combustion. *Appl Energy*. 2018;213:285–92.
- Lyngfelt A, Leckner B, Mattisson T. A fluidized-bed combustion process with inherent CO<sub>2</sub> separation; application of chemical-looping combustion. *Chem Eng Sci*. 2001;56:3101–13.
- Wang S, Wang G, Jiang F, Luo M, Li H. Chemical looping combustion of coke oven gas by using Fe<sub>2</sub>O<sub>3</sub>/CuO with MgAl<sub>2</sub>O<sub>4</sub> as oxygen carrier. *Energy Environ Sci* 2010;3:1353–60.
- Johansson E, Lyngfelt A, Mattisson T, Johnsson F. Gas leakage measurements in a

- cold model of an interconnected fluidized bed for chemical-looping combustion. *Powder Technol* 2003;134:210–7.
- [43] Son SR, Kim SD. Chemical-looping combustion with NiO and Fe<sub>2</sub>O<sub>3</sub> in a thermo-balance and circulating fluidized bed reactor with double loops. *Ind Eng Chem Res* 2006;45:2689–96.
- [44] Shen LH, Wu JH, Xiao J, Song QL, Xiao R. Chemical-looping combustion of biomass in a 10 kW(th) reactor with iron oxide as an oxygen carrier. *Energy Fuels* 2009;23:2498–505.
- [45] Riffart S, Hoteit A, Yazdanpanah MM, Pelletant W, Surla K. Construction and operation of a 10 kW CLC unit with circulation configuration enabling independent solid flow control. *Energy Proc* 2011;4:333–40.
- [46] Antzara A, Heracleous E, Silvester L, Bukur DB, Lemonidou AA. Activity study of NiO-based oxygen carriers in chemical looping steam methane reforming. *Catal Today* 2016;272:32–41.
- [47] Ishida M, Wen CY. Comparison of kinetic and diffusional models for solid-gas reactions. *AIChE J* 1968;14:311–7.
- [48] Jin H, Ishida M. Reactivity study on natural-gas-fueled chemical-looping combustion by a fixed-bed reactor. *Ind Eng Chem Res.* 2002;41:4004–7.
- [49] Kiczek EF. Research and Development of a PEM Fuel Cell, Hydrogen Reformer, and Vehicle Refueling Facility. Air Products and Chemicals, Inc.; 2007. p. Medium: ED; Size: 2.53 MB.